Role and mechanisms of action of microRNA-21 as regards the regulation of the WNT/β-catenin signaling pathway in the pathogenesis of non-alcoholic fatty liver disease

XIU-MEI WANG[1], XIAO-YI WANG[2], YU-MEI HUANG[3], XIA CHEN[3], MU-HAN LÜ[3], LEI SHI[3] and CHANG-PING LI[3]

[1]Department of Gastroenterology, The First People's Hospital of Neijiang, Neijiang, Sichuan 641000; [2]Department of Gastroenterology, The Second People's Hospital of Yibin, Yibin, Sichuan 644000; [3]Department of Gastroenterology, The Affiliated Hospital of Southwest Medical University, Luzhou, Sichuan 646000, P.R. China

Received April 14, 2019; Accepted October 1, 2019

DOI: 10.3892/ijmm.2019.4375

Abstract. The aim of the present study was to investigate the role of *microRNA-21* (*miR-21*) in regulating the classical WNT/β-catenin signaling pathway by targeting low-density lipoprotein-related receptor 6 (LRP6) in non-alcoholic fatty liver disease (NAFLD). For this purpose, we established a NAFLD model by feeding *C57BL/6J* mice a methionine-choline-deficient diet. Antagomir-21 was then injected via the tail vein, and the expression levels of WNT/β-catenin signaling pathway-related proteins, such as LRP6, glycogen synthase kinase-3β (GSK3β), *p*-β-catenin, β-catenin and the downstream protein, peroxisome proliferator-activated receptor γ (PPAR-γ), and lipid metabolism-related genes, including sterol regulatory element-binding transcription factor 1c (*SREBP1c*), fatty acid synthase (*FAS*), carnitine palmitoyl transferase 1α (*CPT1α*) and adenosine 5-monophosphate (AMP)-activated protein kinase α (*AMPKα*), were detected. The results revealed that in the NAFLD model, LRP6 expression was negatively associated with *miR-21* expression. After antagonizing the expression of *miR-21*, the protein level of LRP6 was increased. In addition, the WNT/β-catenin signaling pathway was activated, and lipid accumulation and inflammation were alleviated in the liver. However, the expression of PPAR-γ was not inhibited following the upregulation of the WNT signaling pathway. Taken together, the results of this study demonstrate that the inhibition of *miR-21* expression can alleviate NAFLD by targeting LRP6 to activate the WNT/β-catenin signaling pathway.

Correspondence to: Dr Chang-Ping Li, Department of Gastroenterology, The Affiliated Hospital of Southwest Medical University, 25 Taiping Street, Luzhou, Sichuan 646000, P.R. China
E-mail: 506854209@qq.com

Abbreviations: NAFLD, non-alcoholic fatty liver disease; 1H-MRS, proton magnetic resonance spectroscopy; MRI, magnetic resonance imaging; NAFL, non-alcoholic fatty liver; NASH, non-alcoholic steatohepatitis; C/EBPα, CCAAT enhancer-binding protein α; PPAR-γ, peroxisome proliferator-activated receptor γ; LRP6, low-density lipoprotein-related receptor 6; SREBP1c, sterol regulatory element-binding transcription factor 1c; miR-21, microRNA-21; PPAR-α, peroxisome proliferator activated receptor α; FABP7, fatty acid binding protein 7; HMGCR, 3-hydroxy-3-methylglutaryl coenzyme A reductase; PTEN, phosphate and tension homolog; HBP1D, HMG-box transcription factor 1D; MCD, methionine and choline-deficient; MCS, methionine- and choline-sufficient; ALT, serum alanine aminotransferase; AST, aspartate aminotransferase; TG, triglyceride; TC, total cholesterol; LDL, low-density lipoprotein; FAS, fatty acid synthase; AMPKα, adenosine 5-monophosphate (AMP)-activated protein kinase α; CPT1α, carnitine palmitoyl transferase 1α; GAPDH, glyceraldehyde-3-phosphate dehydrogenase; GSK3β, glycogen synthase kinase-3β; SA, stearic acid; ERK1, extracellular signal-regulated kinase 1; SPRY2, Sprouty2; EMT, epithelial-to-mesenchymal transition; ELOVL, fatty acid elongase; NF-κB, nuclear factor-κB; STAT, signal transducer and activator of transcription; SCAP, SREBP cleavage-activating protein; FXR, farnesoid X receptor

Key words: non-alcoholic fatty liver disease, *microRNA-21*, LRP6, WNT/β-catenin signaling pathway

Introduction

Non-alcoholic fatty liver disease (NAFLD) refers to the excessive accumulation of liver fat according to a histological analysis identifying fatty degeneration in >5% of hepatocytes or a fat fraction density >5.6%, as evaluated by proton magnetic resonance spectroscopy (1H-MRS) or quantitative fat/water selective magnetic resonance imaging (MRI), that leads to subsequent liver injury, balloon-like degeneration, and chronic inflammatory infiltration with or without fibrosis and without excessive alcohol intake (male, <30 g/day, female <20 g/day) or other known causes. NAFLD includes non-alcoholic fatty liver (NAFL) and non-alcoholic steatohepatitis (NASH) (1,2) and has become an epidemic chronic liver disease worldwide (3). However, no specific therapeutic drugs have been developed following decades of research. The reason for this

may be related to several factors, such as the long latency of NAFLD, an incomplete understanding of the pathogenesis of NAFLD (4,5), and the involvement of multiple factors. Further exploration of the molecular mechanisms of NAFLD will contribute to the future development of drugs for the treatment of NAFLD.

The WNT signaling pathway has been classified into the classical and non-classical pathways according to whether the accumulation of β-catenin in the nucleus is necessary or not. The classical WNT/β-catenin signaling pathway has been recognized as a key regulator of adipose differentiation and exerts anti-lipid formation and anti-inflammatory effects. By contrast, the non-classical WNT signaling pathway promotes fat formation, lipid accumulation and inflammation. An imbalance in the WNT signaling pathways has been closely associated with NAFLD. When the classical WNT/β-catenin signaling pathway is activated, the expression of CCAAT enhancer binding protein α (C/EBP-α) and peroxisome proliferator activated receptor γ (PPAR-γ) is inhibited by β-catenin, which in turn inhibits the differentiation of preadipocytes (Fig. 1) (4). A mutation in low-density lipoprotein-related receptor 6 (LRP6; $LRP6^{R611C}$), a common coreceptor of the classical WNT/β-catenin signaling pathway, induces lipid accumulation in the liver through the nutritional sensory pathway [insulin-like growth factor 1 (IGF1)/AKT/mammalian target of rapamycin (mTOR)/sterol regulatory element-binding transcription factor (*SREBP)1/2*] (Fig. 1). Homozygotic $LRP6^{R611C}$ ($LRP6^{mut/mut}$) mice have been shown to exhibit NASH with fibrosis (6,7). Wnt3a is a canonical Wnt ligand (4). As an inhibitor of inflammatory processes, the Wnt3a inhibition of the non-canonical Wnt pathway reduces lipid accumulation and inflammation, but has almost no effect in enhancing the canonical Wnt pathway (7). Along with reducing the influence of the risk factors of NAFLD, it is reasonable to believe that inhibiting the classical WNT/β-catenin regulatory signaling pathway is indispensable in promoting the pathogenesis of NAFLD, and this may be achieved by upregulating PPAR-γ and *SREBP1c*.

MicroRNAs (miRNAs or miRs) are a class of endogenous, single-stranded, non-coding small RNAs with a length of ~19-25 nucleotides that regulate gene expression by inhibiting translation, promoting the cleavage of mRNAs or targeting promoter regions (8). *miR-21* was one of the earliest discovered human miRNAs. In the pathogenesis of NAFLD, *miR-21* has been shown to participate in liver lipid metabolism through a variety of targets, including fatty acid binding protein 7 (FABP7) and 3-hydroxy-3-methylglutaryl coenzyme A reductase (HMGCR), and to contribute to NASH via peroxisome proliferator activated receptor α (PPAR-α). It can also participate in NAFLD through SMAD7, phosphate and tension homolog (PTEN), HMG-box transcription factor 1D (HBP1D) and other targets (8-13). Moreover, our research group previously demonstrated that the expression of LRP6 was inhibited in HepG2 cells transfected with a *miR-21* mimic and that LRP6 was a target of *miR-21*. We also observed that the synthesis of triglycerides was decreased through the inhibition of *miR-21* through RNA interference, suggesting that *miR-21* may be involved in lipid synthesis and metabolism by interacting with the WNT/β-catenin signaling pathway to further participate in the pathogenesis and pathology of NAFLD (14). This was the first time, to the best of our knowledge, that *miR-21* was linked to the WNT/β-catenin signaling pathway. Therefore, in order to explore the regulatory role of *miR-21* in the WNT/β-catenin signaling pathway in NAFLD in mice, the objective of this study was to explore the role of the molecular regulatory network of *miR-21* in the pathogenesis of NAFLD and to elucidate the pathological mechanisms underlying NAFLD.

Materials and methods

Mouse model. All mice were male *C57BL/6J* mice (6 weeks old, n=15, 22.60±1.24 g, purchased from Chengdu Dashuo Laboratory Animal Co., Ltd.; http://www.cd-dossy.cn/) that were bred at the Laboratory Animal Center of Southwest Medical University (http://dwzx.swmu.edu.cn/) and allowed to acclimatize to their environment for 1 week. All animals received care according to the guidelines of the Institutional Animal Care and Use Committee of Southwest Medical University (Luzhou, China), and the experiment was approved by the Experimental Animal Ethics Committee of Southwest Medical University (application acceptance no. 20180521-11). C57BL/6J mice (n=9) were fed a methionine- and choline-deficient diet (MCD, Trophic Animal Feed High-Tech Co., Ltd., http://www.trophic.cn/) to establish NAFLD; after 4 weeks, 3 mice (15.03±0.75 g) without manifestations of peritonitis were sacrificed by cervical dislocation following an intraperitoneal injection of 10% chloral hydrate (400 mg/kg), and the liver tissues were removed for hematoxylin & eosin (H&E) staining to confirm the successful establishment of the model. Subsequently, the remaining mice were divided into 2 groups of 3 mice in each. Antagomir-21 (antagomir-21 group, n=3, 8 mg/kg 5-UCAACACUGUCUGUAGAUCUA-3 (10), purchased from Shanghai Genepharma Pharmaceutical Technology Co. Ltd., http://www.genepharma.bioon.com.cn/) or the same dose of saline (control group, n=3), was injected through the tail vein at 15 weeks of age once a day for 3 consecutive days. The C57BL/6J wild-type mice (normal group, n=6) were fed a methionine- and choline-sufficient diet (MCS, Trophic Animal Feed High-Tech Co. Ltd., http://www.trophic.cn/). After 4 weeks, 3 mice (26.7±0.76 g) without manifestations of peritonitis were randomly selected, anesthetized and sacrificed (using the same method as described above). The liver tissues were removed for H&E staining as a NAFLD control. At 15 weeks of age, the same dose of saline was injected into the tail vein once a day for 3 consecutive days (Fig. 2).

All mice without manifestations of peritonitis (antagomir-21 group, 12.63±0.72 g; control group, 13.4±0.69 g; normal group, 30.13±5.51 g) were anesthetized with 10% chloral hydrate (400 mg/kg) at the age of 19 weeks. Once the mice no longer exhibited a corneal reflex or pain responses, blood (~0.5 ml) was collected from the eyeball and the heart through a needle inserted obliquely into the heart at a 45˚ angle (in the location with the most obvious heartbeat) to obtain blood. After collecting the blood, the mice died within 1 min from continuous cardiac arrest. The collected blood was allowed to settle for 30 min and centrifuged for 20 min at 2,500 x g at 4˚C. The supernatant was collected following centrifugation and stored at -80˚C for blood lipid and aminotransferase detection. The liver was separated quickly and weighed.

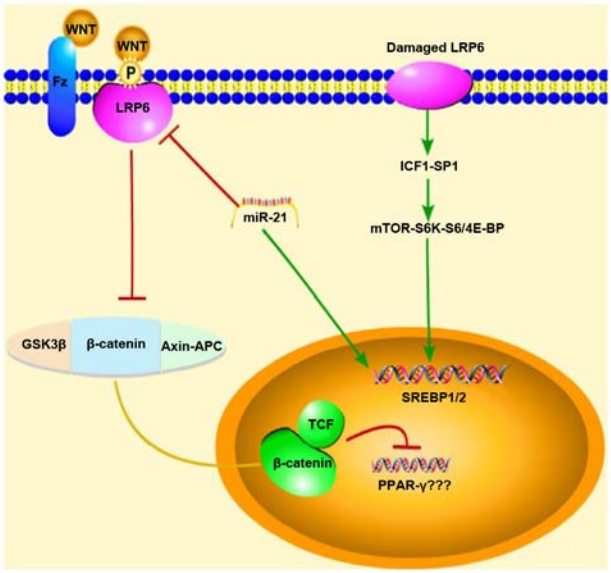

Figure 1. Schematic diagram of the mechanisms of action of *miR-21* showing the regulation of the WNT signaling pathway in NAFLD mice. Red arrows represent inhibition, green arrows represent promotion, and the yellow line represents migration from the cytoplasm into the nucleus When the classical WNT/β-catenin signal is activated, the expression of PPAR-γ is inhibited; however, our experimental results were reversed, and thus, we do not know association between PPAR-γ and the WNT/β-catenin signaling pathway. Thus, due to this uncertainty, question marks (???) were added next to PPAR-γ in the figure. NAFLD, non-alcoholic fatty liver disease; GSK3β, glycogen synthase kinase-3β; LRP6, low-density lipoprotein-related receptor 6; SREBP1/2, sterol regulatory element-binding transcription factor 1/2; IGF1, insulin-like growth factor 1; mTOR, mammalian target of rapamycin.

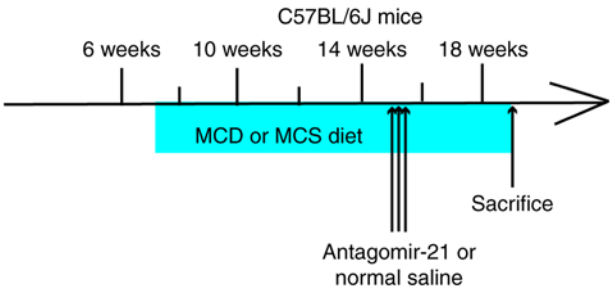

Figure 2. Mouse study design. MCD, methionine- and choline-deficient, MSC, methionine- and choline-sufficient.

Approximately 400 mg of liver tissue were frozen and stored at -80˚C for PCR and western blot analysis. Approximately 300 mg of liver tissue were fixed in 4% formaldehyde for H&E staining and immunohistochemical analysis.

Biochemical analysis. The levels of alanine aminotransferase (ALT), aspartate aminotransferase (AST), triglycerides (TG), total cholesterol (TC) and low-density lipoprotein (LDL) were detected with the DR-200Bs enzyme labeling instrument (Diatek Co., http://www.diateklab.com/) according to the manufacturer's instructions (Nanjing Jiancheng Bioengineering Institute., http://www.njjcbio.com/).

Histological analysis. Paraffin-embedded liver sections (3-μm-thick) were stained with H&E (sent to the Department of Pathology, Affiliated Hospital of Southwest Medical University). The H&E-stained sections were observed under an optical microscope (Olympus, http://www.olympus.com.cn/). The NAS scores of the H&E-stained sections were determined by a pathologist who was blinded to the mouse groupings and according to the following criteria (15): i) Steatosis: 0-3 points, <5, 5-33, 33-66 and ≥66%; ii) intralobular inflammation (counting of necrotic foci at x20 magnification): 0-3 points, none, <2, 2-4, ≥4; and iii) hepatocyte ballooning degeneration change: 0-2 points, none, rare, more common. NASH was excluded by a score of 0-2; NASH could be considered based on a score of 3-4, and NASH would likely be diagnosed based on a score of 5-8.

Western blot analysis. The liver tissues were rinsed 2-3 times with precooled PBS buffer to remove blood, cut into small sections, and placed in a homogenizer (Wuhan Aspen Biotechnology Co., Ltd.). A 10-fold volume of tissue protein extraction reagent (Wuhan Aspen Biotechnology Co., Ltd.) with protease inhibitor (Wuhan Aspen Biotechnology Co., Ltd.) was added and thoroughly homogenized, and the homogenate was incubated in an ice bath for 30 min. The supernatant protein concentration was determined by a BCA protein concentration assay kit (Wuhan Aspen Biotechnology Co., Ltd.) following centrifugation at 4˚C and 13,000 x g for 5 min. The sample size was determined according to the sample concentration, and the total protein in each sample was 40 μg. The protein samples were electrophoretically transferred onto PVDF membranes (Shanghai Millipore Filter Material Co., Ltd., http://millipore.org.cn/search/) after adding an appropriate amount of 5X protein sample buffer (Wuhan Aspen Biotechnology Co., Ltd.) and boiling the samples in a water bath at 95-100˚C for 5 min, in which protein samples were separated using 8-10% SDS-PAGE and the percentage of Tween-20 in TBST was 0.1%. The PVDF membranes were activated with methanol prior to use. The membranes were sealed and incubated at room temperature for 1 h. The sealing fluid was removed, and the membranes were incubated with primary antibody overnight at 4˚C. The diluted primary antibody (Table I) was recovered, and the membranes were washed 3 times with TBST for 5 min each time. The diluted secondary antibody (Table II) was added, and the membranes were incubated at room temperature for 30 min. The membranes were washed in TBST 4 times on a shaker at room temperature for 5 min each time. Freshly mixed ECL solution (Wuhan Aspen Biotechnology Co., Ltd.) was added onto the protein side of the membranes, and the membranes were exposed in a darkroom. The exposure conditions were adjusted to achieve different light intensities prior to developing the film. The photographic films (Eastman Kodak, http://www.kodak.com.cn/) were scanned into files, and the AlphaEaseFC software processing system (Alpha Innotech Corporation, http://www.alphainnotech.com) was used to analyze the optical density of the target bands.

RNA isolation and RT-qPCR analysis. Total RNA was extracted from the liver tissues using a TRIzol reagent kit (Invitrogen™, Semerfly Technology Co., Ltd., https://www.thermofisher.com/), quantified by a SYBR® Premix Ex Taq™ kit (Takara Biomedical Technology Co.,

Table I. Details of primary antibodies used in western blot analysis.

Name of first antibody	Origin	Manufacturer	Cat. no.	Dilution method	Dilution ratio
GAPDH	Rabbit	Abcam	ab37168	5% evaporated milk	1:10,000
LRP6	Rabbit	Abcam	ab134146	5% evaporated milk	1:500
GSK3β	Mouse	Abcam	ab93926	5% evaporated milk	1:1,000
p-β-catenin	Rabbit	Cell Signaling Technology	#4176	5% BSA	1:1,000
β-catenin	Rabbit	Abcam	ab32572	5% evaporated milk	1:3,000
PPAR-γ	Rabbit	Abcam	ab209350	5% evaporated milk	1:500

GAPDH, glyceraldehyde-3-phosphate dehydrogenase; LRP6, low-density lipoprotein-related receptor 6; GSK3β, glycogen synthase kinase-3β; PPAR-γ, peroxisome proliferator activated receptor γ.

Table II. Details of secondary antibodies used in western blot analysis.

Name of secondary antibody	Manufacturer	Cat. no.	Dilution method	Dilution ratio
HRP-goat anti rabbit	KPL	074-1506	5% evaporated milk	1:10,000
HRP-goat anti mouse	KPL	074-1806	5% evaporated milk	1:10,000

Ltd., http://www.takara.com.cn/) according to the manufacturer's instructions and stored at -80˚C. The first-strand cDNA of *miR-21* was synthesized using the M-MLV reverse transcriptase kit (Invitrogen™, Semerfly Technology Co., Ltd., https://www.thermofisher.com/) according to the manufacturer's protocol. The synthesis of the first-strand cDNA for other genes, such as *SREBP1c*, fatty acid synthase (*FAS*), adenosine 5-monophosphate (AMP)-activated protein kinase α (*AMPKα*) and carnitine palmitoyl transferase 1α (*CPT1α*), was performed using the PrimeScriptTM RT Reagent kit with gDNA Eraser (Takara Biomedical Technology Co., Ltd., http://www.takara.com.cn/) according to the manufacturer's protocol. The sequences of the primers are presented in Table III. qPCR was performed on a Life Technologies StepOneTM Real-Time PCR instrument, and each sample was assayed by using 3 replicate wells with the SYBR® Premix Ex TaqTM kit (Takara Biomedical Technology Co., Ltd., http://www.takara.com.cn/). The reaction procedure was as follows: Predenaturation, 95˚C for 1 min; 40 cycles of 95˚C, 15 sec → 58˚C, 20 sec → 72˚C, 45 sec; melting curve, 60˚C → 95˚C, 20 sec per 1˚C of temperature. The reaction conditions were as follows: 2X qPCR Mix, 5.0 μl; primer working dilution (2.5 μM), 1.0 μl; template, 1.0 μl; ddH_2O, 2.8 μl; Rox, 0.2 μl. The corresponding gene expression and relative mRNA expression were evaluated by the $2^{-\Delta\Delta Cq}$ method and the determination of the geometric mean (16).

Immunohistochemistry. Paraffin-embedded sections were placed in a 65˚C oven for 2 h, dewaxed in water, and washed 3 times with PBS (Wuhan Aspen Biotechnology Co., Ltd.) for 5 min each time. The slices were placed in EDTA buffer (Wuhan Aspen Biotechnology Co., Ltd. China) for microwave antigen retrieval, and the microwave was set at medium power until a boil was reached, after which it was set at low power until a boil was reached at intervals of 10 min. After allowing them to cool, the cells were washed with PBS 3 times for 5 min each time. The sections were placed in 3% hydrogen peroxide solution (Sinopharm Chemical Reagent Co., Ltd., https://www.sinoreagent.com/) and incubated for 10 min at room temperature in the dark. The sections were washed 3 times with PBS for 5 min each time and incubated in 5% BSA (Shanghai Roche Pharmaceutical Co., Ltd., https://www.roche.com/) for 20 min after drying. The BSA solution was removed, and ~50 μl of diluted primary antibody (Table IV) was added to each section to cover the tissue, which was incubated at 4˚C overnight. After washing with PBS 3 times for 5 min each time, 50-100 μl of secondary antibody for the corresponding species (Table V) was added to each section, which was incubated for 50 min at 37˚C. The sections were then washed with PBS 3 times for 5 min each time. After removing the PBS solution, 50-100 μl of freshly prepared DAB solution (Beijing Zhongshang Jinqiao Biotechnology Co., Ltd., http://www.zsbio.com/) was added to each section, and the color development was controlled under a microscope (OLYMPUS, Japan, https://www.olympus-global.com). After the color was completely developed, the sections were rinsed with distilled water or tap water, counterstained with hematoxylin (Wuhan Aspen Biotechnology Co., Ltd. China) differentiated with 1% hydrochloric acid in alcohol (approximately 1 sec), rinsed with tap water until the ammonia water turned blue, and then rinsed with water again. The sections were dehydrated with an alcohol gradient (Sinopharm Chemical Reagent Co., Ltd., https://www.sinoreagent.com/) consisting of 75, 90 and 100%, alcohol (10 min each time) and dried, after which they were treated with transparent xylene (Sinopharm Chemical Reagent Co., Ltd., https://www.sinoreagent.com/) and neutral gum (Sinopharm Chemical Reagent Co., Ltd., https://www.sinoreagent.com/) and sealed. The images were magnified at x400 under a microscope (Olympus, https://www.olympus-global.com).

Table III. Sequences of mouse primers used for RT-qPCR.

Primer name	Primer sequence	Product length (bp)
M-GAPDH		
Forward	5'-TGAAGGGTGGAGCCAAAAG-3'	227
Reverse	5'-AGTCTTCTGGGTGGCAGTGAT-3'	
M-SREBP-1c		
Forward	5'-ACAGACAAACTGCCCATCCA-3'	223
Reverse	5'-GCAAGAAGCGGATGTAGTCG-3'	
M-FAS		
Forward	5'-ATCTGGGCTGTCCTGCCTCT-3'	116
Reverse	5'-TTATCAGTTTCACGAACCCGC-3'	
M-AMPKα		
Forward	5'-GATGATGACCATGTGCCAACTC-3'	270
Reverse	5'-CTCCGAACACTCGAACTTCTCAC-3'	
M-CPT1α		
Forward	5'-CATGATTGCAAAGATCAATCGG-3'	141
Reverse	5'-AGCACCTTCAGCGAGTAGCG-3'	
U6		
RT-primer	5'-AACGCTTCACGAATTTGCGT-3'	
Forward	5'-CTCGCTTCGGCAGCACAT-3'	
Reverse	5'-AACGCTTCACGAATTTGCGT-3'	
mmu-miR-21		
RT-primer	*5'-CTCAACTGGTGTCGTGGAGTCGGCAATTCAGTTGAGTCAACATC-3'*	
Forward	5'-ACGGCTTATCAGACTGATGTTGA-3'	
Reverse	5'-CTCAACTGGTGTCGTGGAGTC-3'	

GAPDH, glyceraldehyde-3-phosphate dehydrogenase; *SREBP1-c*, sterol regulatory element-binding transcription factor 1C; *FAS*, fatty acid synthase; *AMPKα*, adenosine 5-monophosphate (AMP)-activated protein kinase α; *CPT1α*, carnitine palmitoyl transferase 1α; *miR-21*, *microRNA-21*.

Table IV. Details of the primary antibodies used for immunohistochemistry.

Name	Species	Manufacturer	Cat. no.	Dilution ratio
LRP6	Goat	Abcam	ab24386	1:200
β-catenin	Rabbit	Abcam	ab32572	1:200
PPAR-γ	Rabbit	Sanying	16643-1-AP	1:300
GSK-3β	Rabbit	Cell Signaling Technology	#12456S	1:400
p-β-catenin	Rabbit	Cell Signaling Technology	#4176	1:100

Table V. Details of the secondary antibodies used for immunohistochemistry.

Name	Manufacturer	Cat. no.	Dilution ratio
HRP-labeled rabbit anti-goat	Aspen	AS-1108	1:200
HRP-labeled goat anti-rabbit	Aspen	AS-1107	1:200

Statistical analysis. The quantitative data were analyzed by SPSS 23.0. All the results are expressed as the means ± SD. One-way ANOVA was used to compare the differences among the groups, followed by the LSD post hoc test. A value of $P<0.05$ was considered to indicate statistically significant differences. The graphics were designed with GraphPad

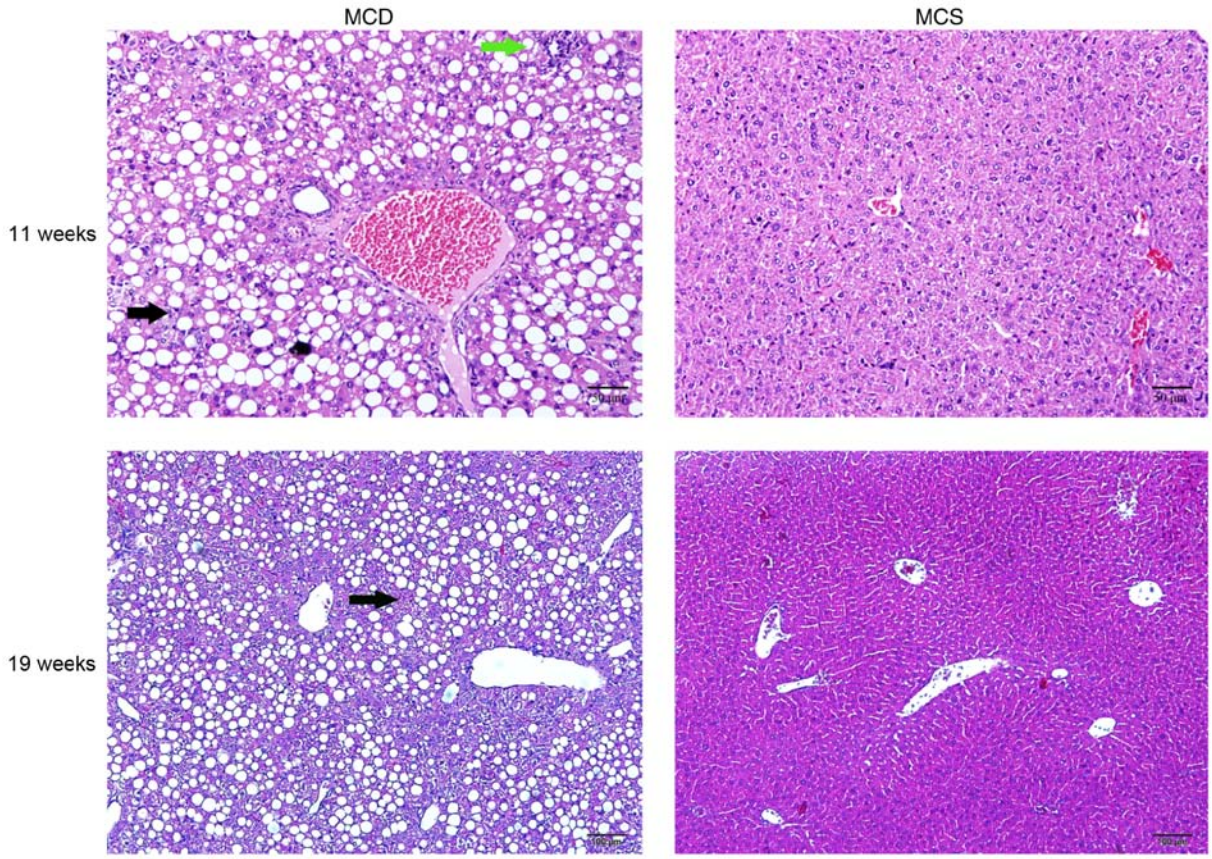

Figure 3. NAFLD was established by feeding an MCD diet to *C57BL/6J* mice. H&E staining at 11 (H&E, x200 magnification) and 19 weeks of age (H&E, x100 magnification). The black arrows indicate steatosis, and the green arrow indicates inflammatory cell infiltration. NAFLD, non-alcoholic fatty liver disease.

Prism 7 Software (GraphPad Software Inc., http://www.graphpad.com/).

Results

Establishment of NAFLD by feeding C57BL/6J mice an MCD diet. After 4 weeks, the livers from the *C57BL/6J* mice fed an MCD diet were examined by H&E staining, which revealed an increase in steatosis and inflammatory cell infiltration in the MCD *C57BL/6J* group compared with the normal group, and the normal structure of the hepatic lobules was disordered. However, hepatic fibrosis was not observed. After continuously feeding the mice an MCD diet until they reached 19 weeks of age, hepatic fibrosis was not observed (Fig. 3).

Expression of miR-21 is significantly increased in C57BL/6J mice fed an MCD diet. After feeding the mice the MCD diet, the expression of *miR-21* in the livers of mice in each group was detected, and *miR-21* expression was markedly increased in the mice fed the MCD diet (control group) compared with that in the MCS group (normal group) at 19 weeks of age. Furthermore, antagomir-21 was injected via the tail vein, and the level of *miR-21* in the livers of the mice was markedly lower than that in the control group (Fig. 4A). In addition, hepatic steatosis and inflammation in the mice fed the MCD and injected with antagomir-21 (Fig. 4C) were significantly reduced compared with the control group (Fig. 4D).

Inhibition of miR-21 expression improves lipogenesis and transaminase levels in C57BL/6J mice fed an MCD diet. In mice fed the MCD diet, the levels of serum lipids (TG, TC and LDL), transaminases (ALT and AST) and genes related to lipid synthesis (*SREBP1c* and *FAS*) were significantly higher than those in the normal mice fed the MCS diet, while the expression of genes related to lipid oxidation (*AMPKα* and *CPT1α*) in the MCD group was relatively lower than that in the normal group. Following the injection of antagomir-21, the blood lipid and transaminase levels were improved, the expression of lipid synthesis-related genes was inhibited, however, the expression of lipid oxidation genes was increased (Figs. 5 and 6).

Inhibition of MIR-21 expression activates the WNT/β-catenin signaling pathway in NAFLD. To validate the regulatory role of *miR-21* in the WNT signaling pathway in mice with NAFLD, antagomir-21 was injected via the tail vein into mice fed the MCD diet, and the same amount of saline was used as a control. Western blot analysis and immunohistochemical staining were used to detect the expression of classical WNT/β-catenin signaling pathway-related proteins in the liver. By inhibiting the expression of *miR-21*, the protein levels of LRP6 were increased compared to those in the control group. Moreover, the expression of glycogen synthase kinase-3β (GSK3β), a downstream degradation complex protein, was reduced, and the accumulation of β-catenin was increased in the cytoplasm. Furthermore, the activity of PPAR-γ, a downstream target

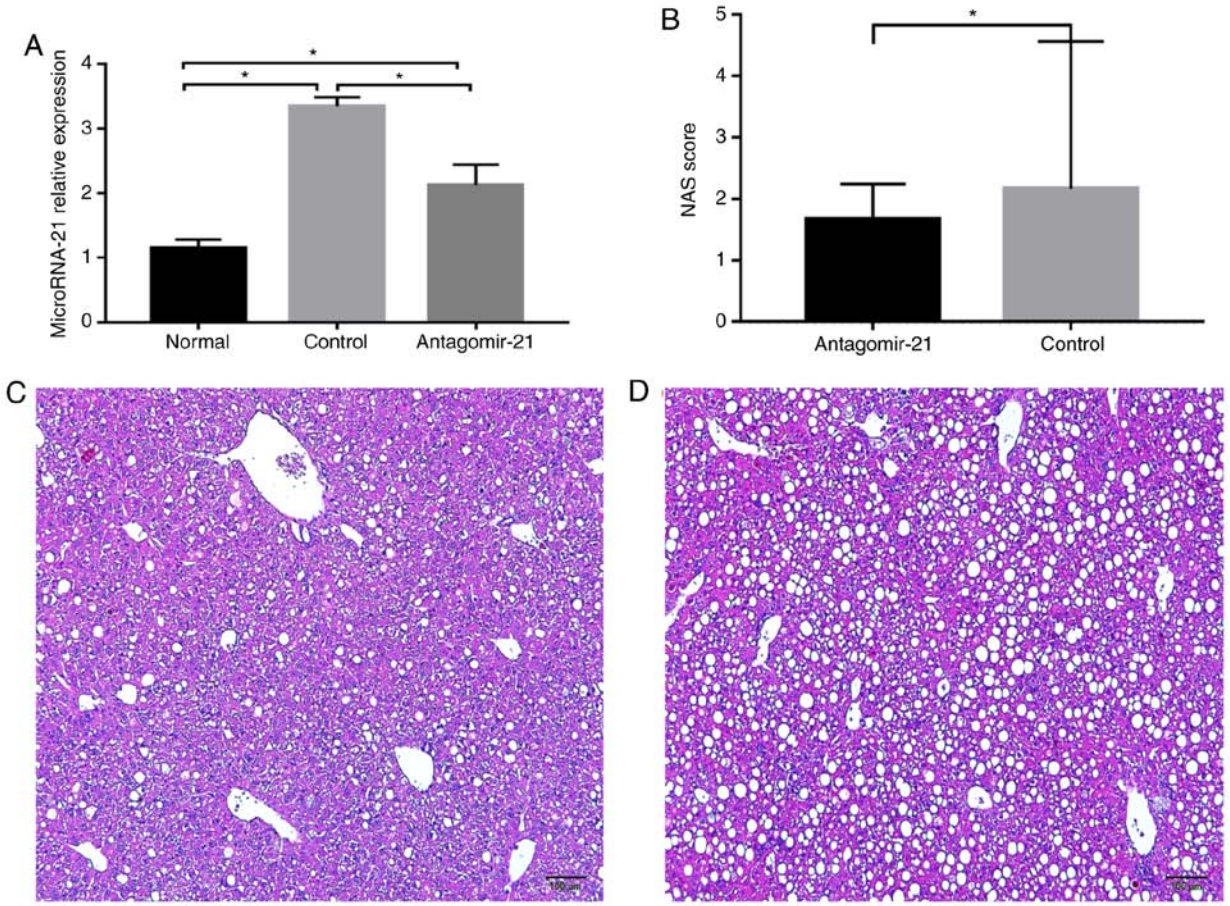

Figure 4. Expression of *miR-21* and H&E staining in the liver following the injection of antagomir-21 into *C57BL/6J* mice. (A) Expression of *miR-21* in each group of mice; (B) NAS scoring of the liver sections. (C) Antagomir-21 group H&E staining of the livers of the mice at 19 weeks of age (H&E, x100 magnification). (D) Control group H&E staining of the livers of the mice at 19 weeks of age (H&E, x100 magnification). *P<0.05.

of the WNT/β-catenin signaling pathway, was not inhibited following the activation of the WNT signaling pathway, but was in fact increased (Figs. 7 and 8).

Discussion

The MCD diet has commonly been used for the establishment of NAFLD models, and steatosis and steatohepatitis are usually evident after feeding for 4 weeks (17). Due to the simplicity and rapid development of the MCD model, we used the MCD diet to establish a NAFLD model, and we observed evidence of NAFLD in our experiments. As one of the miRNAs associated with the pathogenesis and progression of NAFLD, *miR-21* has exhibited alterations in its expression associated with NAFLD. Ahn *et al* found that the expression level of *miR-21* in the livers of mice with steatosis induced by a high-fat diet (49.29% of total fat calories) was lower than that in the control group, and that the expression of *miR-21* was also downregulated *in vitro* by cultivating Hepa 1-6 cells in saturated fatty acids, including stearic acid (SA) (8), and this is consistent with the results observed in insulin-resistant and diabetic mice with NAFL induced by a high-fat diet (18) and in patients with NAFLD (9). However, other studies have demonstrated that serum *miR-21* levels in patients with NAFL are significantly higher than those in healthy individuals and are increased with the increasing severity of fatty liver, although the correlation has not been found to be statistically significant (19). A previous study by Becker *et al* found that there was no significant difference in the expression of *miR-21* in serum from patients with NAFL and healthy individuals (20). In this study, we established a model of NAFLD by feeding *C57BL/6J* mice an MCD diet and found that the expression of *miR-21* in the liver was increased by ~3-fold compared to that in the liver in the normal group that was fed the MCS diet. The discrepancy in the expression of *miR-21* in different research models of NAFLD could be explained by the experimental results of Loyer *et al*, who found that *miR-21* was mainly expressed in inflammatory cells and bile duct cells, but was not expressed as much in the liver (10).

In the model of NAFLD in this study, the livers of mice exhibited evidence of steatosis, the infiltration of inflammatory cells and damage to hepatocytes. The inhibition of *miR-21* expression in mice alleviated steatosis and inflammation due to NAFLD, which is consistent with other research results (10,21). Transaminase and lipid levels in the blood were also improved, and the expression of lipid metabolism genes was also ameliorated following the inhibition of *miR-21*. Antagomir-21 could be used as a treatment method. Thus far, whether therapy targeting *miR-21* can alleviate liver fibrosis has not yet been determined. *miR-21* may participate in the process of liver fibrosis through its effects on multiple targets by inhibiting SMAD7 via the TGF-β/SMAD7 signaling

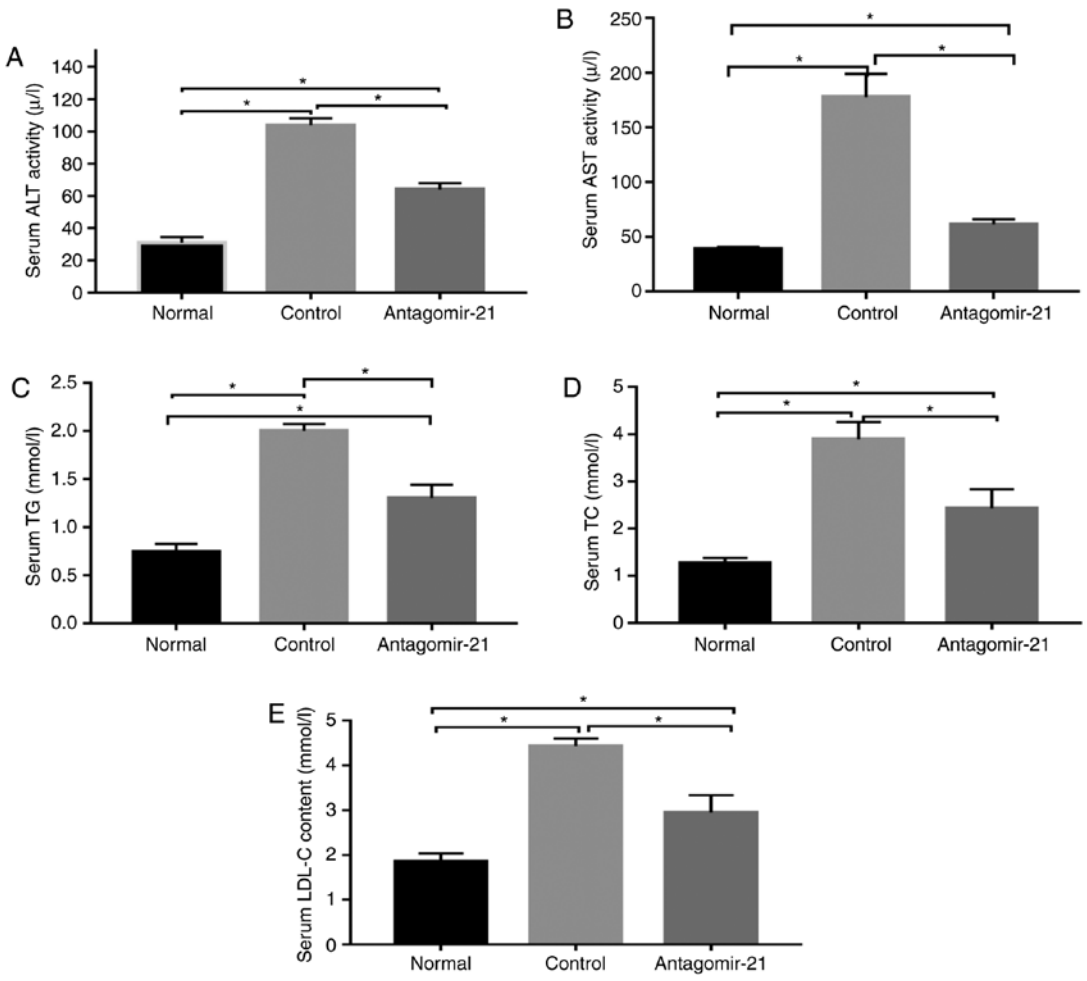

Figure 5. Serum lipid and transaminase levels changed following the injection of antagomir-21 into *C57BL/6J* mice. The (A) serum ALT, (B) AST, (C) TG, (D) TC, and (E) LDL levels were reduced following the injection of antagomir-21. *P<0.05. ALT, alanine aminotransferase; AST, aspartate aminotransferase; TG, triglycerides; TC, total cholesterol; LDL, low-density lipoprotein.

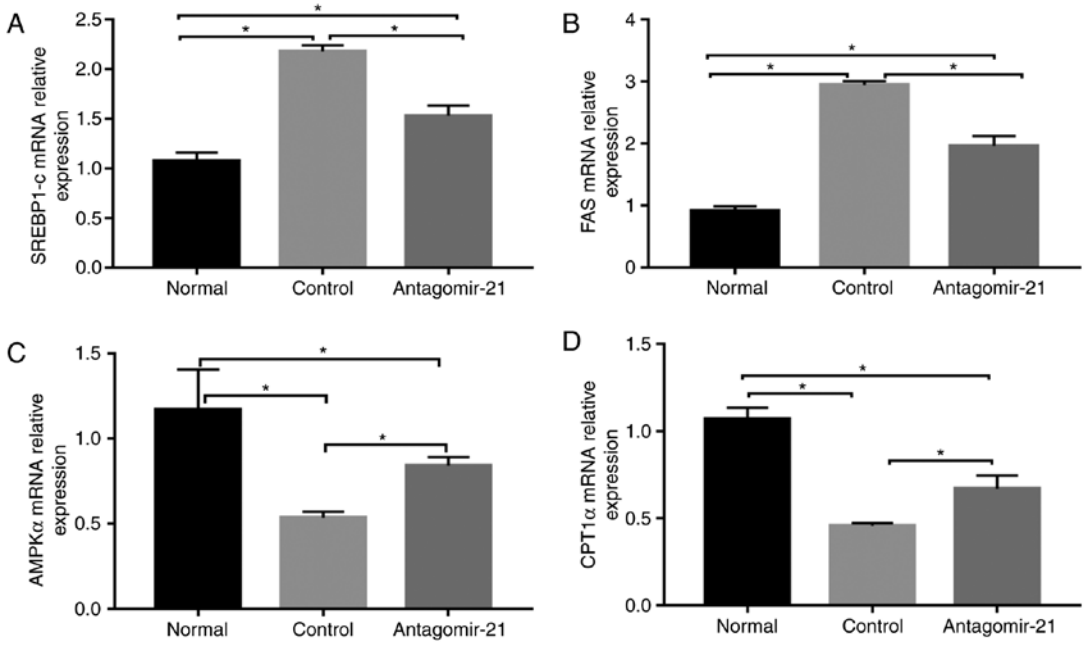

Figure 6. The mRNA levels of lipid metabolism-related genes following the injection of antagomir-21 into the livers of *C57BL/6J* mice. (A-D) *SREBP1c*, *FAS*, *AMPKα* and *CPT1α* mRNA levels were ameliorated in *C57BL/6J* mice fed an MCD diet following the injection of antagomir-21 compared to the control mice injected with saline. *P<0.05. *SREBP1c*, sterol regulatory element-binding transcription factor 1C; FAS, fatty acid synthase; *AMPKα*, adenosine 5-monophosphate (AMP)-activated protein kinase α; *CPT1α*, carnitine palmitoyl transferase 1α.

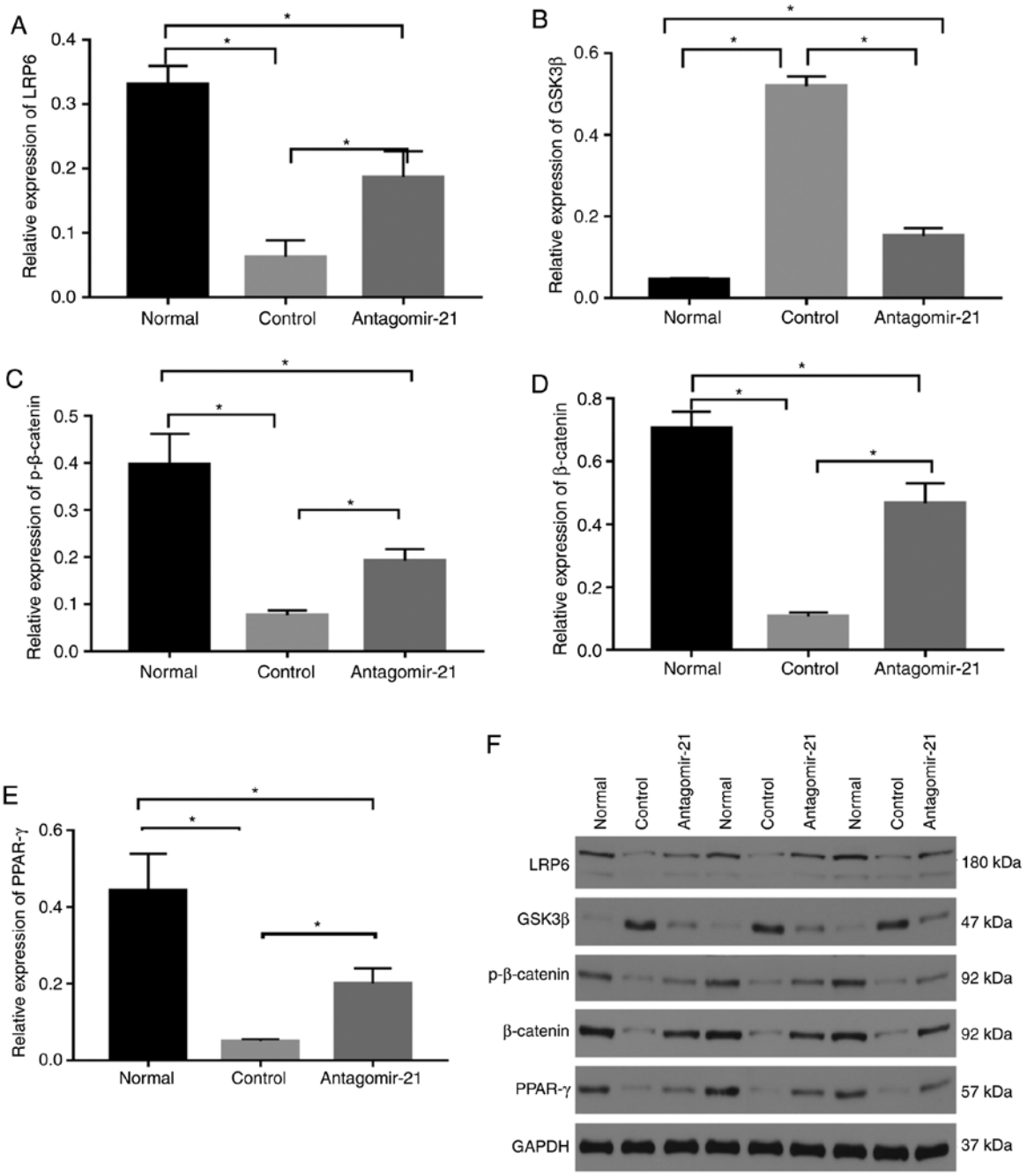

Figure 7. Regulatory effects of *mi-21* on the WNT/β-catenin signaling pathway in NAFLD. Western blot analysis was performed to compare protein levels. (A) The levels of LRP6 protein were inhibited in mice fed the MCD diet, which was upregulated by antagomir-21. (B) Protein levels of GSK3β were higher in the control group and lower in the antagomir-21 group. (C) Protein levels of p-β-catenin were lower in the control group and higher in the antagomir-21 group. (D) Protein levels of β-catenin were lower in the control group and higher in the antagomir-21 group. (E) Protein levels of PPAR-γ were lower in the control group and higher in the antagomir-21 group. (F) Expression levels of LRP6, pβ-catenin, β-catenin, PPAR-γ were inhibited, and the expression of GSK3β was increased in mice fed the MCD diet; antagomir-21 administration exerted opposite effects. *P<0.05. NAFLD, non-alcoholic fatty liver disease; MCD, methionine and choline-deficient; GSK3β, glycogen synthase kinase-3β; LRP6, low-density lipoprotein-related receptor 6; PPAR-γ, peroxisome proliferator-activated receptor γ.

pathway (11) and activating the extracellular signal-regulated kinase 1 (ERK1) signaling pathway by inhibiting SPROUTY2 (SPRY2) to promote epithelial-to-mesenchymal transition (EMT) (22). However, the results from the study by Caviglia *et al* demonstrated that the inhibition of *miR-21* did not prevent the development of liver fibrosis (23).

LRP6 participates in the endocytosis of lipoproteins (6). It has been recognized that the dysfunction of LRP6, such as that caused by the LRP6 gene mutation LRP6^{R611C} (R611C: rs121918313), is involved in dyslipidemia and NAFLD. LRP6^{R611C} mice exhibit hyperlipidemia and liver lipid accumulation, lipid synthesis genes, such as *SREBP1c* and *SREBP2*, and regulated downstream lipases, including acetyl coenzyme A carboxylase, *FAS*, *SCD1*, diglyceryl transferase 1 and the elongation of very long chain fatty acids [fatty acid elongase (*ELOVL*)] family members, are increased in LRP6^{R611C} mice (6). Similarly, Montazeri-Najafabady *et al* recently demonstrated that the LRP6^{V1062I} polymorphism (V1062I: rs2302685) was

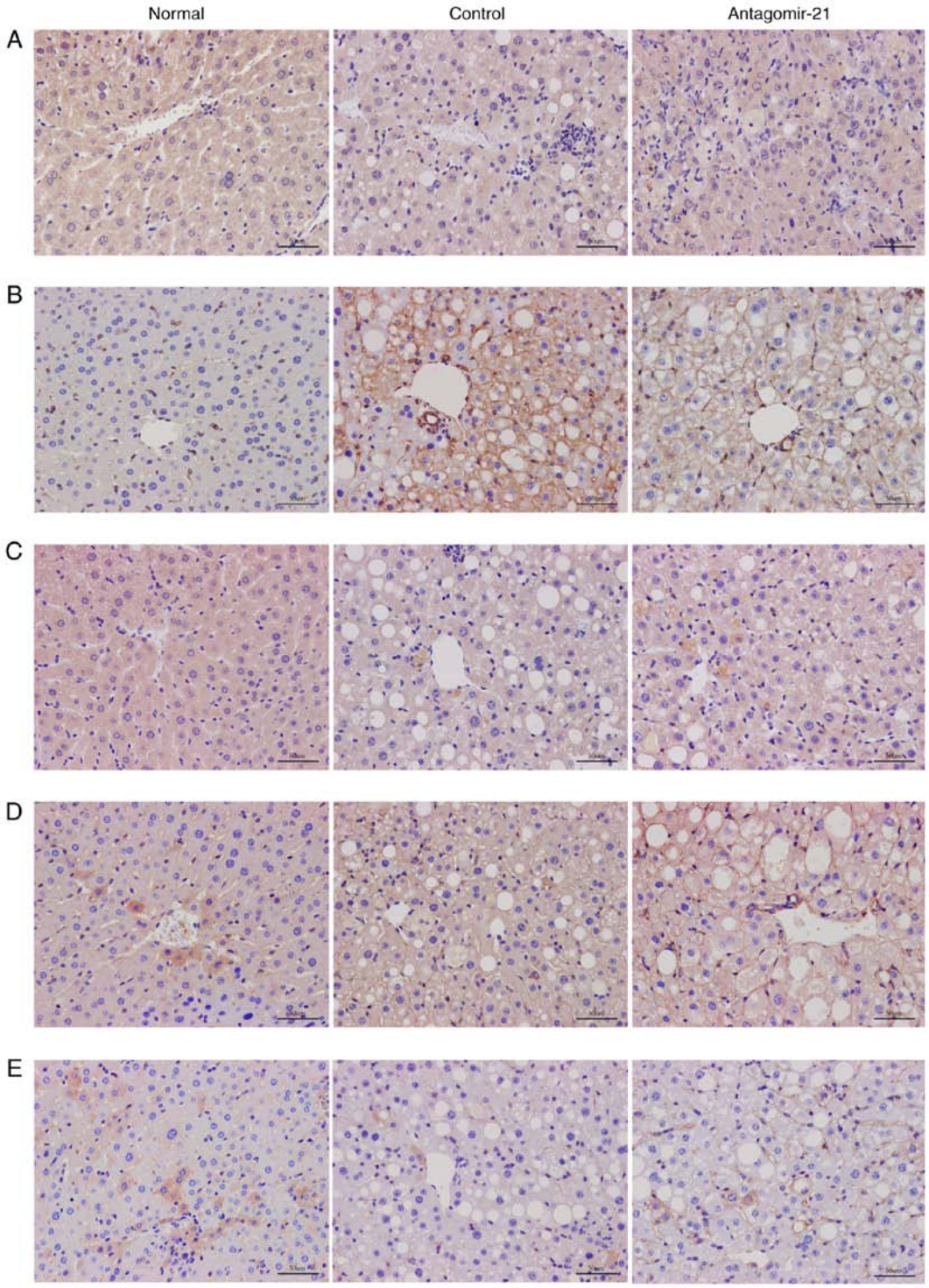

Figure 8. Immunohistochemical results for the WNT signaling pathway. The expression levels of (A) LRP6, (B) GSK3β, (C) p-β-catenin, (D) β-catenin and (E) PPAR-γ were detected by immunohistochemical staining in the normal group, control group and antagomir-21 group.

associated with an increased risk of hyperlipidemia in Iranian children and adolescents, which also increased the risk of elevated total cholesterol, TG, LDL and non-HDL levels (24). By using rmWnt3a, the blood lipid levels of LRP6^{R611C} mice and the enzymes involved in lipid *de novo* synthesis can be normalized (25). These results indicate that LRP6 can be utilized as a therapeutic target for the treatment of NAFLD by regulating the WNT/β-catenin signaling pathway. In a previous study by our group, the overexpression of *miR-21* in hepatocytes inhibited the expression of LRP6 (14). In the mouse experiments in this study, we observed that LRP6 expression was increased, which activated the WNT/β-catenin signaling pathway, decreased the degradation of β-catenin and caused more β-catenin to translocate to the nucleus to regulate the expression of target genes, such as PPAR-γ, following the inhibition of the expression of *miR-21* in the livers of mice (Fig. 1). However, in contrast to previous research (6), in this study, the level of PPAR-γ was increased compared with that in the control group. This may be related to

the regulation of *miR-21*. Some studies have shown that PPAR-γ is negatively associated with the expression of *miR-21* (18), however, whether it is a target of *miR-21* has yet to be determined. PPAR-γ can induce preadipocyte differentiation, promote adipogenesis, induce adipocytes to absorb and store free fatty acids, and promote the transfer of liver fat to adipocytes, at the same time, PPAR-γ activation alleviates inflammation via its negative interaction with nuclear factor-κB (NF-κB) and signal transducer and activator of transcription (STAT), and promotes macrophage cell transition to M2 to inhibit the development of NAFLD (26), for example, the agonist, rosiglitazone, has been shown to prevent NASH progression in animal models induced by dietary methionine choline deficiency. The antagonistic expression of *miR-21* may alleviate NASH steatosis and inflammation by regulating the WNT/β-catenin signaling pathway in addition to negatively regulating other targets, such as PPAR-α (10).

In addition to PPAR-γ, *miR-21* may also regulate *SREBP1c* via the WNT signaling pathway. *SREBP1c* promotes the *de novo* synthesis of fat and adipogenesis. *SREBP1/2* is normally retained in the endoplasmic reticulum through Insig1 and Insig2, activated by AKT, transported to the Golgi apparatus via SREBP cleavage-activating protein (*SCAP*) to induce protein hydrolysis and maturation, and then ectopically transferred to the nucleus, in which it binds to target genes (25). *miR-21* regulates the expression of *SREBP1c* through the *Hbp1-p53-Srebp1c* pathway (13). $LRP6^{R611C}$ also participates in the progression of NAFLD through the nutritional *IGF1-AKT-mTOR-SREBP1/2* pathway. In this study, we also verified the expression of *SREBP1c* and the expression level of the downstream target, *FAS*. After *miR-21* expression was reduced, LRP6 was activated, and *SREBP1c* was inhibited. The expression levels of the *CPT1α* and *AMPKα* genes, which are related to lipolysis, were increased, and thereby NAFLD was attenuated. Therefore, *miR-21* can regulate the expression of *SREBP1c*-related lipid metabolism genes through the WNT/β-catenin signaling pathway. Due to limited funding, this study did not examine the effects of inhibiting *miR-21*, while antagonizing LRP6 expression or activating LRP6 expression with other drugs in NAFLD. Simultaneously, if *miR-21* knockout mice can be used instead of *miR-21* inhibitors to treat mice, perhaps better results would be obtained.

Further limitations to this study include the small numbers of mice, the simple design of the experiment and the lack of an appropriate control. However, in spite of these, this study demonstrates that the inhibition of *miR-21* expression in mice attenuated NASH steatosis and inflammation, partly by targeting the coreceptor LRP6 and activating the WNT/β-catenin signaling pathway. This finding was consistent with that of a previous cell study (14), which further supported our hypothesis that *miR-21* may participate in the pathogenesis of NAFLD via its regulation of the WNT/β-catenin signaling pathway; this has enriched our understanding of the molecular mechanisms of *miR-21* in NAFLD. This finding also supported the possibility of inhibiting *MIR-21* expression as a treatment for NAFLD. Due to the complexity of the pathogenesis of NAFLD and the influence of lifestyle habits, single-target therapy has not achieved satisfactory results. miRNAs have multitarget characteristics and can be regulated by multiple miRNAs. Although the inhibition of *miR-21* alone may not achieve satisfactory results, the targeting of *miR-21* could also enhance the therapeutic efficacy of other drugs, such as a combination of *miR-21* and the farnesoid X receptor (FXR) agonist obeticholic acid (21), and the complex molecular mechanism network underlying the involvement of *miR-21* in NAFLD warrants further investigation. In the future, multitarget drug combinations may become an option for NAFLD treatment.

Acknowledgements

Not applicable.

Funding

The study was supported by a grant from the Affiliated Hospital of Southwestern Medical University Research Project-General Project in 2017 (grant no. 17172), which was awarded to Dr Chun Yang who was responsible for the funding for this study.

Availability of data and materials

All data generated or analyzed during this study are included in this published article.

Authors' contributions

XMW, XYW and CPL were involved in the conception, design and review the manuscript in the study. XMW and XYW were involved in the writing and revising of the original draft. XMW, XYW and YMH were involved in data collection and statistical analysis. XC, LS and MHL were responsible for experimental method operation, resource procurement and fund management. All authors read and approved the final manuscript.

Ethics approval and consent to participate

All animals received humane care according to the guidelines of the Institutional Animal Care and Use Committee of Southwest Medical University, and the experiment was approved by the Experimental Animal Ethics Committee of Southwest Medical University (application acceptance no. 20180521-11).

Patient consent for publication

Not applicable.

Competing interests

The authors declare that they have no competing interests.

References

1. Hardy T, Oakley F, Anstee QM and Day CP: Nonalcoholic fatty liver disease: Pathogenesis and disease spectrum. Annu Rev Pathol 11: 451-496, 2016.
2. Cai J, Zhang XJ and Li H: Progress and challenges in the prevention and control of nonalcoholic fatty liver disease. Med Res Rev 39: 328-348, 2019.
3. Fiorucci S, Biagioli M and Distrutti E: Future trends in the treatment of non-alcoholic steatohepatitis. Pharmacol Res 134: 289-298, 2018.

4. Ackers I and Malgor R: Interrelationship of canonical and non-canonical Wnt signalling pathways in chronic metabolic diseases. Diab Vasc Dis Res 15: 3-13, 2018.
5. Green CJ, Parry SA, Gunn PJ, Ceresa CDL, Rosqvist F, Piché ME and Hodson L: Studying non-alcoholic fatty liver disease: The ins and outs of in vivo, ex vivo and in vitro human models. Horm Mol Biol Clin Investig Aug 11, 2018 (Epub ahead of print).
6. Go GW: Low-density lipoprotein receptor-related protein 6 (LRP6) is a novel nutritional therapeutic target for hyperlipidemia, non-alcoholic fatty liver disease, and atherosclerosis. Nutrients 7: 4453-4464, 2015.
7. Wang S, Song K, Srivastava R, Dong C, Go GW, Li N, Iwakiri Y and Mani A: Nonalcoholic fatty liver disease induced by noncanonical Wnt and its rescue by Wnt3a. FASEB J 29: 3436-3445, 2015.
8. Ahn J, Lee H, Jung CH and Ha T: Lycopene inhibits hepatic steatosis via microRNA-21-induced downregulation of fatty acid-binding protein 7 in mice fed a high-fat diet. Mol Nutr Food Res 56: 1665-1674, 2012.
9. Sun C, Huang F, Liu X, Xiao X, Yang M, Hu G, Liu H and Liao L: miR-21 regulates triglyceride and cholesterol metabolism in non-alcoholic fatty liver disease by targeting HMGCR. Int J Mol Med 35: 847-853, 2015.
10. Loyer X, Paradis V, Hénique C, Vion AC, Colnot N, Guerin CL, Devue C, On S, Scetbun J, Romain M, *et al*: Liver microRNA-21 is overexpressed in non-alcoholic steatohepatitis and contributes to the disease in experimental models by inhibiting PPARα expression. Gut 65: 1882-1894, 2016.
11. Dattaroy D, Pourhoseini S, Das S, Alhasson F, Seth RK, Nagarkatti M, Michelotti GA, Diehl AM and Chatterjee S: Micro-RNA 21 inhibition of SMAD7 enhances fibrogenesis via leptin-mediated NADPH oxidase in experimental and human nonalcoholic steatohepatitis. Am J Physiol Gastrointest Liver Physiol 308: G298-G312, 2015.
12. Wei J, Feng L, Li Z, Xu G and Fan X: MicroRNA-21 activates hepatic stellate cells via PTEN/Akt signaling. Biomed Pharmacother 67: 387-392, 2013.
13. Wu H, Ng R, Chen X, Steer CJ and Song G: MicroRNA-21 is a potential link between non-alcoholic fatty liver disease and hepatocellular carcinoma via modulation of the HBP1-p53-Srebp1c pathway. Gut 65: 1850-1860, 2016.
14. Li CP, Li HJ, Nie J, Chen X and Zhou X: Mutation of miR-21 targets endogenous lipoprotein receptor-related protein 6 and nonalcoholic fatty liver disease. Am J Transl Res 9: 715-721, 2017.
15. Kleiner DE, Brunt EM, Van Natta M, Behling C, Contos MJ, Cummings OW, Ferrell LD, Liu YC, Torbenson MS, Unalp-Arida A, *et al*: Design and validation of a histological scoring system for nonalcoholic fatty liver disease. Hepatology 41: 1313-1321, 2005.
16. Livak KJ and Schmittgen TD: Analysis of relative gene expression data using real-time quantitative PCR and the 2(-Delta Delta C(T)) method. Methods 25: 402-408, 2001.
17. Kong M, Chen X, Xu H, Wenping, Fang M and Xu Y: Hepatocyte-specific deletion of Brg1 alleviates methionine-and-choline-deficient diet (MCD) induced non-alcoholic steatohepatitis in mice. Biochem Biophys Res Commun 503: 344-351, 2018.
18. Zhao XY and Shao K: Roles of microRNA-21 in the pathogenesis of insulin resistance and diabetic mellitus-induced non-alcoholic fatty liver disease. Zhongguo Yi Xue Ke Xue Yuan Xue Bao 38: 144-149, 2016 (In Chinese).
19. Yamada H, Suzuki K, Ichino N, Ando Y, Sawada A, Osakabe K, Sugimoto K, Ohashi K, Teradaira R, Inoue T, *et al*: Associations between circulating microRNAs (miR-21, miR-34a, miR-122 and miR-451) and non-alcoholic fatty liver. Clin Chim Acta 424: 99-103, 2013.
20. Becker PP, Rau M, Schmitt J, Malsch C, Hammer C, Bantel H, Müllhaupt B and Geier A: Performance of serum microRNAs -122, -192 and -21 as biomarkers in patients with non-alcoholic steatohepatitis. PLoS One 10: e0142661, 2015.
21. Rodrigues PM, Afonso MB, Simão AL, Carvalho CC, Trindade A, Duarte A, Borralho PM, Machado MV, Cortez-Pinto H, Rodrigues CM and Castro RE: miR-21 ablation and obeticholic acid ameliorate nonalcoholic steatohepatitis in mice. Cell Death Dis 8: e2748, 2017.
22. Wu K, Ye C, Lin L, Chu Y, Ji M, Dai W, Zeng X and Lin Y: Inhibiting miR-21 attenuates experimental hepatic fibrosis by suppressing both the ERK1 pathway in HSC and hepatocyte EMT. Clin Sci (Lond) 130: 1469-1480, 2016.
23. Caviglia JM, Yan J, Jang MK, Gwak GY, Affo S, Yu L, Olinga P, Friedman RA, Chen X and Schwabe RF: MicroRNA-21 and Dicer are dispensable for hepatic stellate cell activation and the development of liver fibrosis. Hepatology 67: 2414-2429, 2018.
24. Montazeri-Najafabady N, Dabbaghmanesh MH and Mohammadian Amiri R: The association of LRP6 rs2302685 (V1062I) polymorphism with the risk of hyperlipidemia in Iranian children and adolescents. Ann Hum Genet 82: 382-388, 2018.
25. Go GW, Srivastava R, Hernandez-Ono A, Gang G, Smith SB, Booth CJ, Ginsberg HN and Mani A: The combined hyperlipidemia caused by impaired Wnt-LRP6 signaling is reversed by Wnt3a rescue. Cell Metab 19: 209-220, 2014.
26. Silva AKS and Peixoto CA: Role of peroxisome proliferator-activated receptors in non-alcoholic fatty liver disease inflammation. Cell Mol Life Sci 75: 2951-2961, 2018.